

Grain boundary engineering of titanium-stabilized 321 austenitic stainless steel

K. Kurihara · H. Kokawa · S. Sato ·

Y. S. Sato · H. T. Fujii · M. Kawai

Received: 27 September 2010/Accepted: 30 December 2010/Published online: 19 January 2011
© Springer Science+Business Media, LLC 2011

Abstract Grain boundary engineering (GBE) primarily aims to prevent the initiation and propagation of intergranular degradation along grain boundaries by frequent introduction of coincidence site lattice (CSL) boundaries into the grain boundary networks in materials. It has been reported that GBE is effective to prevent intergranular corrosion due to sensitization in unstabilized 304 and 316 austenitic stainless steels, but the effect of GBE on intergranular corrosion in stabilized austenitic stainless steels has not been clarified. In this study, a twin-induced GBE utilizing optimized thermomechanical processing with small pre-strain and subsequent annealing was applied to introduce very high frequencies of CSL boundaries into a titanium-stabilized 321 austenitic stainless steel. The resulting steel showed much higher resistance to intergranular corrosion after sensitization subsequent to carbon re-dissolution heat treatment during the ferric sulfate–sulfuric acid test than the as-received one. The high CSL frequency resulted in a very low percolation probability of random boundary networks in the over-threshold region

and remarkable suppression of intergranular corrosion during GBE.

Introduction

Intergranular degradation often limits the lifetime and reliability of polycrystalline structural materials. In spite of persistent efforts to suppress such degradation, its complete prevention has not yet been achieved. Intergranular corrosion due to sensitization of austenitic stainless steels is a conventional and momentous problem during high temperature use and welding, such as weld decay [1]. Sensitization is caused by chromium depletion due to chromium carbide precipitation at grain boundaries. Conventional methods for preventing sensitization of austenitic stainless steels include reduction of carbon content in the material, stabilization of carbon atoms as non-chromium carbides by the addition of titanium or niobium with higher affinity to carbon than chromium, local solution-heat-treatment by laser beam, etc. These methods, however, are not without drawbacks. For example, knife line corrosion attacks the weld heat affected zone (HAZ) of stabilized austenitic stainless steels due to sensitization, since carbon which has been stably retained by titanium or niobium as TiC or NbC in stabilization heat treatment is re-dissolved in the HAZ during welding thermal history [1].

Grain boundary studies have revealed that grain boundary phenomena strongly depend on the grain boundary structure and character [2–6]. It is generally accepted that low-energy boundaries such as coincidence site lattice (CSL) boundaries, are highly resistant to deterioration, as contrasted with high-energy boundaries such as random boundaries. The concept of “grain boundary design and control” [7] has been developed and refined as grain boundary engineering (GBE) [8]. GBE primarily aims to prevent the initiation and

K. Kurihara · H. Kokawa (✉) · S. Sato ·

Y. S. Sato · H. T. Fujii

Department of Materials Processing, Graduate School of Engineering, Tohoku University, 6-6-02 Aramaki-aza-Aoba, Aoba-ku, Sendai 980-8579, Japan
e-mail: kokawa@material.tohoku.ac.jp

Present Address:

S. Sato

Advanced Technology Research Laboratories, Nippon Steel Corporation, 20-1 Shintomi, Futtu 293-8511, Japan

M. Kawai

Institute of Materials Structure Science, High Energy Accelerator Research Organization, Oho, Tsukuba-shi, Ibaraki-ken 305-0801, Japan

propagation of intergranular degradation along random boundaries by frequent introduction of CSL boundaries into the grain boundary networks in materials. Recent GBE investigations [9–22] have been promoting a new innovative approach for suppression of the intergranular degradation phenomena such as intergranular cracking, intergranular corrosion, etc., which can lead to destruction of polycrystalline material structures before their design service life. Many GBE investigations have dealt with face-centered cubic materials with low stacking fault energy which leads to frequent generation of annealing twins. Suitable thermomechanical processing increases the frequency of CSL boundaries and results in a desirable grain boundary character distribution (GBCD) with disconnected random boundaries being produced in the material by twin-emissions and boundary–boundary reactions during annealing [12, 16]. Optimized GBCD has demonstrated a high resistance to intergranular corrosion due to sensitization in austenitic stainless steels [12, 16–18]. A recent review [23] of the twinning-related GBE introduced many grain boundary engineered materials (GBEMs) which showed improvement in properties. The review states that the highest frequency (87%) of CSL boundaries in structural materials was achieved by the GBE of a 304 austenitic stainless steel [12]. The GBEM of 304 stainless steel also has an advantage in that the high CSL frequency was obtained by one-step thermomechanical processing, in contrast with the other GBE processes [2, 4, 8–11] which require several iterations of strong strain plus annealing for favorable GBCD or improvement of material properties. Michiuchi et al. [16] have also reported that one-step thermomechanical processing introduced a high frequency of CSL boundaries into 316 austenitic stainless steel and consequently decreased the susceptibility to intergranular corrosion significantly.

The previous studies have demonstrated that GBE is effective for preventing intergranular corrosion by sensitization due to intergranular carbide precipitation in unstabilized 304 and 316 austenitic stainless steels [12, 16, 17]. Meanwhile, titanium or niobium-stabilized austenitic stainless steels cause intergranular corrosion due to sensitization after exposure to enough high temperatures to re-dissolve stabilized carbides (TiC or NbC), such as knife line corrosion of welding [1]. GBE may probably be also effective to suppress the intergranular corrosion in stabilized austenitic stainless steels. This study aimed to examine the effect of GBE on the intergranular corrosion in a titanium-stabilized 321 austenitic stainless steel.

Experimental

The material used in this study was a stabilized type 321 austenitic stainless steel. The chemical composition (wt%)

was 17.47 Cr, 9.41 Ni, 0.49 Si, 0.84 Mn, 0.04 C, 0.024 P, 0.001 S, and 0.35 Ti. The as-received 321 steel, solution-heat treated at 1323 K for 0.5 h, was termed the starting base material (321BM) in this study. The 321BM, 9 × 10 × 35 mm³ in size, was thermomechanically processed by one-step pre-strain plus annealing [12, 16]. The pre-strain was given by cold-rolling, resulting in a 0–5% reduction of specimen thickness. The ranges of annealing temperatures and time were 1220–1300 K for 72 h. The thermomechanically processed 321 steel specimens were annealed at 1173 K for 1 h to stabilize carbon as TiC by titanium so as to prevent chromium carbide precipitation. The specimen which achieved an optimum GBCD with the highest frequency of CSL boundaries was termed as grain boundary engineered material (321GBEM) in this article.

The GBCD were analyzed by electron backscatter diffraction (EBSD) using a HITACHI SE-4300SE field emission scanning electron microscope (SEM) after stabilization heat treatment at 1173 K for 1 h with thermomechanically processed specimens. The frequency of CSL boundaries was cited as a percentage by length on the cross-sections perpendicular to the specimen surface. Brandon's criterion [24] was adopted for the critical deviation in the grain boundary characterization [25]. Although the relationship between the grain boundary energy and the Σ value is not simple depending on the grain boundary plane, etc., the present authors reported that the grain boundaries with $\Sigma \leq 29$ CSL misorientations were prone to show higher resistance to intergranular carbide precipitation and corrosion than the other grain boundaries in a sensitized 304 austenitic stainless steel [6, 15]. Therefore, in this study, grain boundaries with $\Sigma \leq 29$ were classified as CSL boundaries with low energy, the others being classified as random boundaries with high energy, since special properties have been reported in CSL boundaries with $\Sigma \leq 29$ [6, 8].

The intergranular corrosion properties of the stabilized 321BM and 321GBEM were evaluated by a ferric sulfate–sulfuric acid test [26] after sensitization treatment at 923 K for 24 h subsequent to TiC solution heat treatment at 1673 K for 300 s. The intergranular corrosion susceptibility was assessed to measure the weight loss of the specimens for a period of test time during the ferric sulfate–sulfuric acid test. The surface and cross-section of the ferric sulfate–sulfuric acid tested specimens were observed by SEM.

Results and discussion

Production of GBEM by thermomechanical processing

Previous studies [12, 16] have obtained GBEed austenitic stainless steels by one-step thermomechanical processing

consisting of slight pre-strain and subsequent annealing for 72 h, in which GBCDs indicate extremely high CSL frequencies over 85%. In addition, the parameters of thermomechanical processing, especially pre-strain and annealing temperature, would affect GBCD intricately. The combined effects of pre-strain and annealing temperature on CSL frequency of the thermomechanically processed 321 austenitic stainless steel after stabilization heat treatment are shown in Fig. 1. These specimens were produced by annealing at 1220–1300 K for 72 h, after 1–5% pre-strain in thickness. The CSL frequency in the thermomechanically processed specimens after stabilization shows a maximum CSL frequency of 89% around 3% pre-strain and annealing at 1260 K for 72 h. The three-dimensional (3D) distribution of the optimized GBCD with the high CSL frequency through the specimen thickness of about 9 mm was confirmed in the 321GBEM by EBSD analysis of cross-sections perpendicular the specimen surface. Since the maximum CSL frequency of 89% is comparably high to 304 and 316GBEMs in previous studies [12, 16], the specimen with the maximum CSL frequency of 89% for 321 steel was regarded as 321GBEM. The EBSD-GBCD maps of 321BM (a) and 321GBEM (b) after stabilization are indicated in Fig. 2. In these maps, black and gray lines indicate random and CSL boundaries, respectively. Average grain sizes including all boundaries in Fig. 2 are 9 and 19 μm for 321BM (a) and 321GBEM (b), respectively. Continuous networks of random boundaries uniformly developed in the 321BM (Fig. 2a), where the CSL frequency was 53%. On the other hand, the random boundary network was disrupted and fragmented by the high density of CSL boundaries (over 85%) in the 321GBEM (Fig. 2b).

Figure 3 shows the fractions in length of Σ CSL boundaries for 321BM (a) and 321GBEM (b). Higher fractions of $\Sigma 3$ and $\Sigma 9$ boundaries in 321GBEM (Fig. 3b) than those in 321BM (Fig. 3a) suggest frequent formation of annealing twins and active twin-twin reactions during the thermomechanical processing for GBE. Consequently, the 321GBEM (Fig. 3b) includes a number of $\Sigma 3^n$ CSL boundaries where n is integer. The previous study [12] reported that random boundaries partly transformed the grain boundary structures from random to CSL by emission of annealing twins and that the transformed segments showed high corrosion resistant in thermomechanically processed austenitic stainless steels. Since an annealing twin formation generally reduces the grain boundary energy during grain growth [27], the grain boundary energy of the part where the twin was emitted is likely to be lower than that of the initial random boundary. Formation of an annealing twin can introduce a low energy segment into the random high angle grain boundary and can sometimes result in low- Σ CSL structures. Active twin events and reactions increase the frequency of CSL boundaries and also

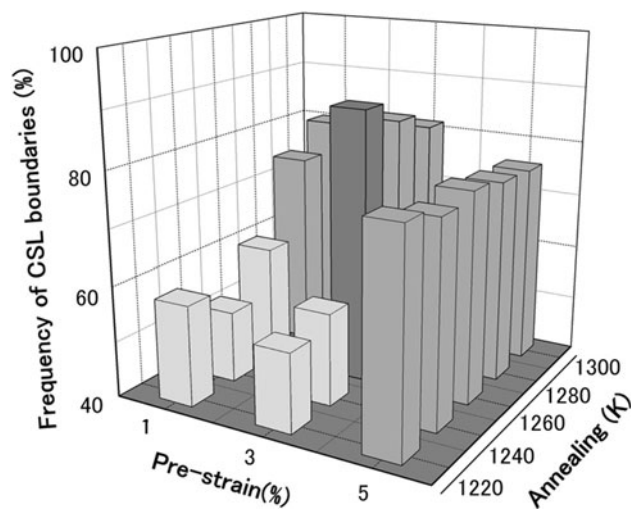


Fig. 1 Effects of pre-strain and annealing temperature on the frequency of CSL boundaries in thermomechanically processed 321 austenitic stainless steel

frequently produce low energy segments in high-energy boundaries locally during thermomechanical processing of low stacking fault energy materials such as austenitic stainless steels [12]. An analytical TEM observation has demonstrated that the chromium depletion at a CSL segment introduced by twin emission into a random boundary was significantly suppressed compared with that of the original random boundary during sensitization [13]. Well-distributed low energy segments in the grain boundary network create a discontinuous chain of chromium depletion and can arrest the percolation of intergranular corrosion from the surface [12]. A small pre-strain is probably more suitable for an optimum distribution of non-corrosive segments than large pre-strains, because a large pre-strain tends to promote recrystallization which generates corrosive random boundaries and also CSL boundaries while a small pre-strain accelerates grain growth accompanying twins without generation of new random boundaries during thermomechanical processing [12]. The small pre-strain activates grain boundary migration without new grain generation. A migrating grain boundary inevitably interacts with lattice dislocations and other grain boundaries during grain growth. Because of the reactions, a low-energy boundary cannot move a long distance, because the absorption rate of lattice dislocation by a low energy boundary is much lower than that of a random boundary [28] and the migration never occurs before completion of the absorption [29]. Also, the reactions possibly change the grain boundary structures to lower energy ones at high temperatures [3]. A low energy structure is stable and resistant to interactions with defects [30]. Therefore, a low energy boundary tends not to move, while a high energy boundary can migrate widely and consequently has a great

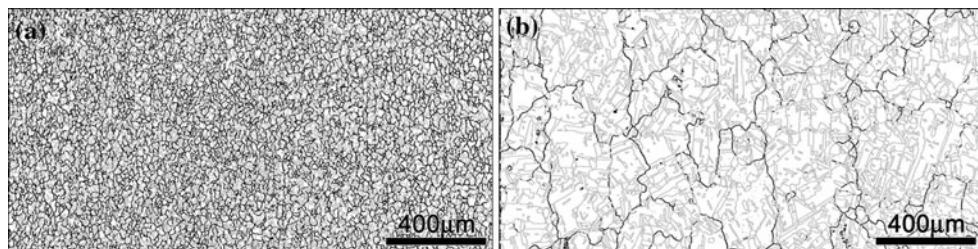


Fig. 2 EBSD-GBCD maps of 321BM (a) and 321GBEM (b). Black and gray lines indicate random and CSL boundaries, respectively

opportunity for interaction with other boundaries or twin emissions so as to produce new low energy segments. Once low energy boundary segments are produced, they tend to survive for a long time. In the strain annealing, the small strain introduced by rolling promotes grain growth and subsequently preferentially initiates the high CSL frequency layer near the specimen surface, and the layer grows into the specimen interior inversely along the strain gradient [12]. Abnormal grain growth at a relatively low temperature may also play a very important role in the evolution of optimized GBCD, because a small number of random boundaries migrate widely for a long time and interact effectively with other boundaries [12]. On the other hand, normal grain growth at higher temperatures cannot effectively disrupt the random boundary network, because of the simultaneous, short migration of many random boundaries [12].

Intergranular corrosion resistance of GBEM

In order to simulate the region where knife line corrosion attacks in the weld HAZ, the stabilized 321BM and 321GBEM were TiC-solution heat treated at 1673 K for 300 s so as to re-dissolve carbon. Figure 4 shows EBSD-GBCD maps of 321BM (a) and 321GBEM (b) after the solution heat treatment at 1673 K. The solution heat treatment brought grain growth which led to average grain sizes of 34 and 46 μm and to CSL frequencies of 64 and 85% in the 321BM and 321GBEM, respectively. The optimized GBCD with the high CSL frequency was maintained in the 321GBEM during the high temperature exposure. The high thermal stability of the optimized

GBCD was reported also in HAZ of 304GBEM during welding [17].

Subsequently the 321BM and 321GBEM were heat treated at 923 K for 24 h for sensitization. Then, the ferric sulfate–sulfuric acid test was carried out to examine the intergranular corrosion resistance of the 321BM and 321GBEM. Intergranular corrosion propagates along grain boundaries and causes mass-loss due to grain dropping from the material surface. The result of the ferric sulfate–sulfuric acid test is shown in Fig. 5. The corrosion (mass-loss) rate of 321GBEM was much lower than that of 321BM during the ferric sulfate–sulfuric acid test. The surface and cross-sectional (perpendicular to cold-rolling direction) microstructures after the ferric sulfate–sulfuric acid test for 120 h were observed by SEM, as presented in Fig. 6. Although intergranular corrosion is more or less seen on the surfaces of both 321BM and 321GBEM subjected to the long-term test, the cross-sectional observations show much less grain-dropping in the 321GBEM than in the 321BM. GBE ensures excellent intergranular corrosion resistance due to sensitization even after carbon redissolution in the stabilized austenitic stainless steel, compared with the 321BM not subjected to GBE.

The excellent intergranular corrosion resistance of 321GBEM is resulted from the optimized GBCD which is described as an uniform distribution of a high frequency of CSL boundaries and consequent discontinuity of the random boundary network in the material. Intergranular corrosion preferentially propagates from the surface into the interior of the specimen along the random boundaries. The resistance by GBE to intergranular corrosion depends on the degree of connectivity of random boundaries, i.e., less

Fig. 3 Fractions of Σ CSL boundaries for 321BM (a) and 321GBEM (b)

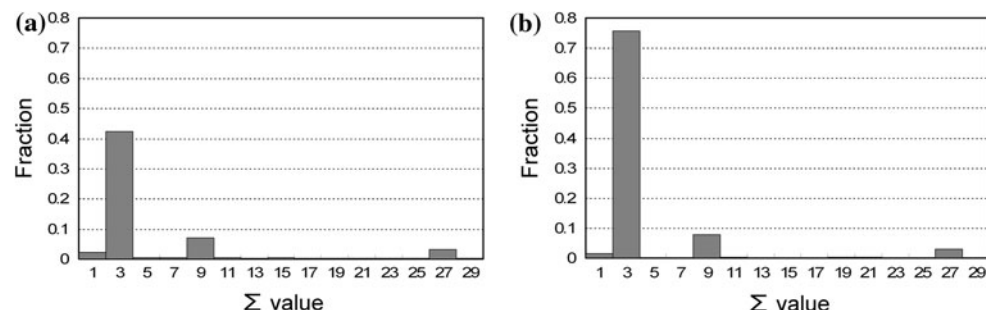


Fig. 4 EBSD-GBCD maps of 321BM (a) and 321GBEM (b) after the heat treatment at 1673 K for 300 s. Black and gray lines indicate random and CSL boundaries, respectively

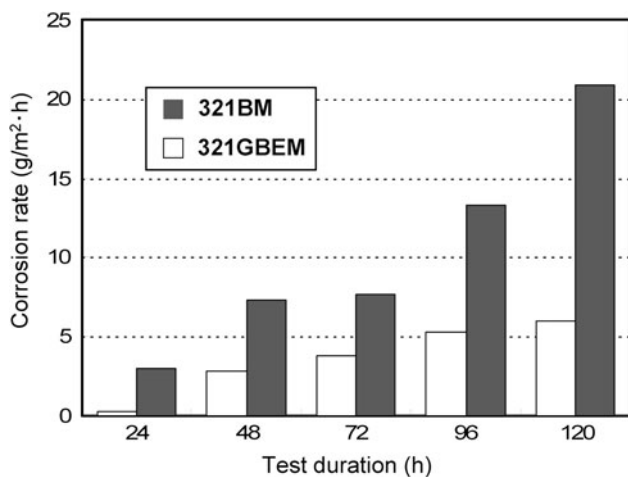
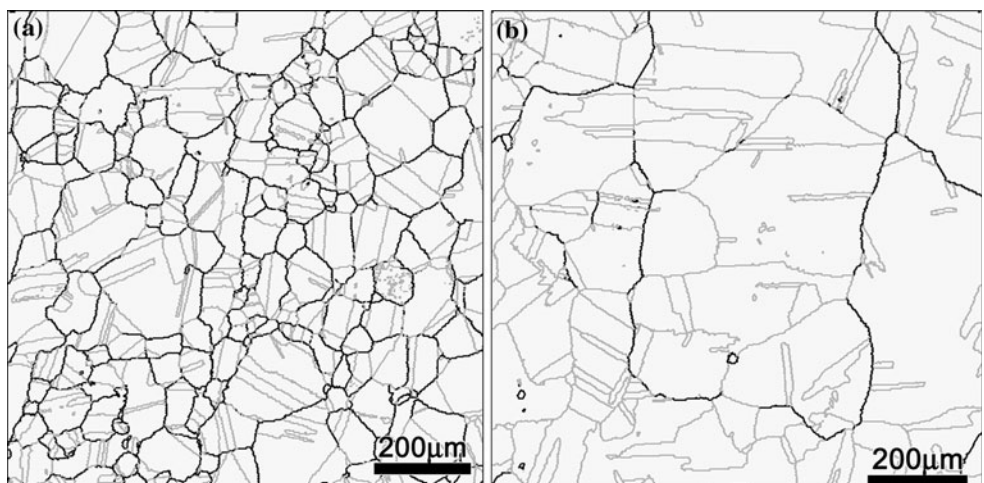


Fig. 5 Corrosion rates of stabilized 321BM and 321GBEM after sensitization treatment at 923 K for 24 h subsequent to TiC solution heat treatment at 1673 K for 300 s during the ferric sulfate–sulfuric acid test

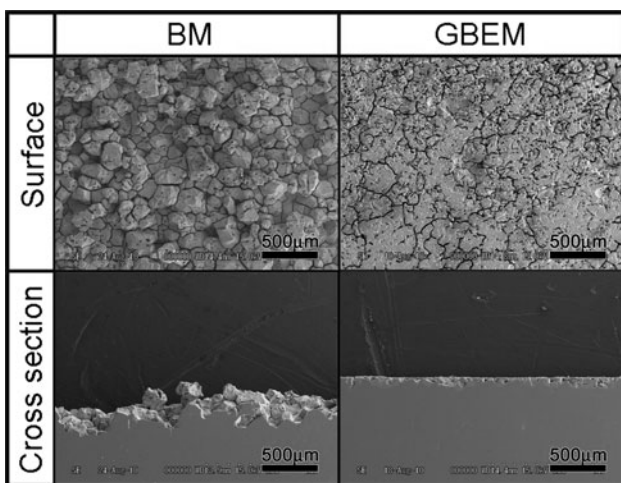


Fig. 6 The surfaces and cross-sections of 321BM and 321GBEM after the ferric sulfate–sulfuric acid test for 120 h

connectivity is more desirable. The degree of connectivity can be quantified using the percolation theory with a cluster of random boundaries [31, 32]. The percolation probability of random boundaries decreases with an increase in the frequency of CSL boundaries and indicates a sharp drop at a threshold of CSL frequency [32–34]. The two-dimensional (2D) percolation in austenitic stainless steels has been experimentally reported to be about 70% of CSL frequency [16, 34]. The 2D percolation probability of random boundaries in the 321GBEM measured with the EBSD-GBCD map of Fig. 2b was 0.063 which is as low as those in the 304GBEM and 316GBEM in the previous studies [16, 19]. Wells et al. [33] estimated that 2D and 3D percolation thresholds of susceptible grain boundary clusters in an austenitic stainless steel are about 35 and 77%, respectively, in the frequency of susceptible grain boundaries on the basis of the simple binary random bond percolation theory. The 2D percolation threshold of about 70% in the previous studies [16, 34] is much higher than 35%. Random bond percolation, however, cannot be simply applied to twin-induced GBE, because the GBCD produced by twin-induced GBE is under crystallographic constraints at triple junctions according to the Σ -product rule [35]. Schuh et al. [32] showed that as compared with randomly assembled networks, about 50–75% more resistant boundaries will be required to fragment the susceptible grain boundaries in 2D GBCD when the Σ -product rule is adapted to the simulation. Frary et al. [36] estimated the 3D percolation threshold in crystallographic constrained grain boundary networks to be 80% in CSL frequency for the twinned microstructure where $\Sigma 3^n$ CSL boundaries are special. The high CSL frequencies over 85% in the 321GBEM (even after TiC-solution heat treatment at 1673 K for 300 s) exceeded the threshold, even considering that it included about 2% of non- $\Sigma 3^n$ CSL frequency ($\Sigma \leq 29$). However, it should be noted that the frequency of CSL boundaries is somewhat higher than that of

corrosion-resistant boundaries because the CSL boundaries did not always resist corrosion well in the 321GBEM as generally mentioned by Randle [37]. However, these results of the ferric sulfate–sulfuric acid test experimentally revealed that a CSL frequency over 85% is also significantly effective to suppress intergranular corrosion in a stabilized 321 austenitic stainless steel even after carbon re-dissolution, and support the theoretical estimation by Frary et al. [36] that the 3D percolation threshold of random boundaries is 80% of the CSL frequency in austenitic stainless steels. A CSL frequency of over 80% may assure the very low percolation probability of random boundary networks in the over-threshold region, as well as remarkable suppression of intergranular deterioration during twin-induced GBE of austenitic stainless steels. Although consideration of grain boundary planes [37, 38] and other factors may probably give the precise frequency of corrosion-resistant boundaries, the frequency of CSL boundaries is an available and statistical parameter to evaluate the degree of GBE at present.

Conclusions

One-step thermomechanical-processing of titanium-stabilized 321 austenitic stainless steels produced 321GBEM with the optimized GBCD which is described as an uniform distribution of a high frequency of CSL boundaries over 85% and consequent discontinuity of the random boundary network. The optimized GBCD was maintained even after carbon re-dissolution heat treatment at 1673 K for 300 s. The stabilized 321GBEM demonstrated much higher resistance to intergranular corrosion due to sensitization subsequent to carbon re-dissolution than the corresponding 321BM during the ferric sulfate–sulfuric acid test. A CSL frequency of over 80% may assure very low percolation probability of random boundary networks in the over-threshold region and remarkable suppression of intergranular deterioration during twin-induced GBE of stabilized 321 austenitic stainless steel.

Acknowledgements This work was supported by a Grant-in-Aid for Scientific Research (A) (No. 21246104), a Grant-in-Aid for Science Research (S) (No. 19106013), a Grant-in-Aid for Science Research (S) (No. 19106017), and a grant from the Global COE Program “Materials Integration (International Center of Education and Research), Tohoku University.” MEXT, Japan. The authors wish to thank to Mr. E. Nagashima and Mr. A. Honda for their technical assistance and useful discussion.

References

1. Folkhard E (1984) Welding metallurgy of stainless steels. Springer, Wien
2. Le Coze J, Biscondi M (1974) Can Metall Quart 13:59
3. Kokawa H, Watanabe T, Karashima S (1981) Philos Mag A 44:1239
4. Qian XR, Chou YT (1982) Philos Mag A 45:1075
5. Kokawa H, Lee CH, North TH (1991) Metall Trans A 22:1627
6. Kokawa H, Shimada M, Sato YS (2000) JOM 52(7):34
7. Watanabe T (1984) Res Mech 11:47
8. Palumbo G, Lehockey EM, Lin P (1998) JOM 50(2):40
9. Spigarelli S, Cabibbo M, Evangelista E, Palumbo G (2003) Mater Sci Eng A 352:93
10. Qian M, Lippold JC (2003) Acta Mater 51:3351
11. Randle V, Davies H (2002) Metall Mater Trans A 33:1853
12. Shimada M, Kokawa H, Wang ZJ, Sato YS, Karibe I (2002) Acta Mater 50:2331
13. Bi HY, Kokawa H, Wang ZJ, Shimada M, Sato YS (2003) Scripta Mater 49:219
14. Kokawa H, Shimada M, Wang ZJ, Sato YS, Michiuchi M (2004) Key Eng Mater 261–263:1005
15. Kokawa H (2005) J Mater Sci 40:927. doi:[10.1007/s10853-005-6511-6](https://doi.org/10.1007/s10853-005-6511-6)
16. Michiuchi M, Kokawa H, Wang ZJ, Sato YS, Sakai K (2006) Acta Mater 54:5179
17. Kokawa H, Shimada M, Michiuchi M, Wang ZJ, Sato YS (2007) Acta Mater 55:5401
18. Jin WZ, Yang S, Kokawa H, Wang ZJ, Sato YS (2007) J Mater Sci Technol 23:785
19. Yang S, Wang ZJ, Kokawa H, Sato YS (2007) J Mater Sci 42:847. doi:[10.1007/s10853-006-0063-2](https://doi.org/10.1007/s10853-006-0063-2)
20. Xia SA, Zhou BX, Chen WJ (2008) J Mater Sci 43:2990. doi:[10.1007/s10853-007-2164-y](https://doi.org/10.1007/s10853-007-2164-y)
21. Krupp U (2008) J Mater Sci 43:3908. doi:[10.1007/s10853-007-2363-6](https://doi.org/10.1007/s10853-007-2363-6)
22. Jin WZ, Kokawa H, Wang ZJ, Sato YS, Hara N (2010) ISIJ Intern 50:476
23. Randle V (2004) Acta Mater 52:4067
24. Brandon DG (1966) Acta Metall 14:1479
25. Kokawa H, Watanabe T, Karashima S (1987) Scripta Metall 21:839
26. Lee JB (1983) Corrosion 39:469
27. Fullman RL, Fisher JC (1951) J Appl Phys 22:1350
28. Kokawa H, Watanabe T, Karashima S (1983) J Mater Sci 18:1183. doi:[10.1007/BF00551977](https://doi.org/10.1007/BF00551977)
29. Pumphrey PH, Gleiter H (1974) Philos Mag 30:593
30. Kokawa H, Watanabe T, Karashima S (1983) Scripta Metall 17:1155
31. Schuh CA, Kumar M, King WE (2003) Acta Mater 51:700
32. Schuh CA, Minich RW, Kumar M (2003) Philos Mag 83:711
33. Wells DB, Stewart J, Herbert AW, Scott PM, Williams DE (1989) Corrosion 45:649
34. Tsurekawa S, Nakamichi S, Watanabe T (2006) Acta Mater 54:3617
35. Miyazawa K, Iwasaki Y, Ito K, Ishida Y (1996) Acta Crystallogr A 52:787
36. Frary M, Schuh CA (2005) Philos Mag 85:1123
37. Randle V (2006) Scripta Mater 54:1011
38. Randle V, Jones R (2009) Mater Sci Eng A 524:134